

Energy-Aware Random Access Networks: Connection-Based versus Packet-Based

Anshan Yuan , Fangming Zhao , Xinghua Sun , *Member, IEEE*

Abstract—Characterizing and comparing the optimal energy efficiency in energy-aware machine-to-machine (M2M) random access networks remains a challenge due to the distributed nature of the access behavior of nodes. To address this issue, this letter focuses on the energy efficiency limits of two typical random access schemes, i.e., connection-based Aloha and packet-based Aloha, based on which we conducted a performance comparison. Specifically, by integrating limited energy constraints and network throughput, the lifetime throughput can be derived, and further optimized with a guarantee of targeted lifetime via selecting the transmission probability. Then we present a comparative study on the optimal lifetime throughput of packet-based Aloha and connection-based Aloha to characterize criteria for beneficial connection establishment.

Index Terms—Energy efficiency, Random Access, connection-based, packet-based, lifetime throughput, slotted Aloha.

I. INTRODUCTION

The rapid expand of Machine-Type Devices (MTDs) has notably enhanced the prevalence of machine-to-machine (M2M) communications. With the high volume of MTDs, M2M data transmission faces challenges arising from frequent channel access collisions and increased energy consumption. Moreover, in M2M network, nodes are usually battery-operated without recharging ability, resulting in a stringent constraint on energy consumption. Impractical transmission strategies may also shorten the communication lifetime of MTDs, detrimentally impacting the long-term functionality of the network. Consequently, energy efficiency becomes a crucial metric for M2M network [1], [2].

Since the dense MTDs and complicated transmission process in the M2M network result in frequent collisions and unnecessary energy waste, 3GPP recognizes the adoption of MTDs utilizing 2-step (connection-free) and 4-step (connection-based) Random Access Small Data Transmission (RA-SDT) strategies in M2M networks [3]. This approach aims to streamline the transmission process to improve throughput and energy efficiency. To investigate the throughput performance of the RA-SDT mechanism, the Aloha protocol, known for its simplicity, compared with other existing multiple access technology [4], [5], still has exhibited significant potential in theoretical exploration and adapting the high volume of MTDs. Aloha is divided into two types based on

its transmission methodology: packet-based Aloha (PB-Aloha) and connection-based Aloha (CB-Aloha), corresponding to the 2-step RA-SDT and the 4-step RA-SDT, respectively [6], [7].

In PB-Aloha, nodes directly transmit data packets, while in CB-Aloha, nodes initially send a shorter preamble to compete for channel access. Intuitively, PB-Aloha incurs higher energy waste and low network throughput in failed data transmissions. Yet, the energy overhead of the preamble and delay created by the connection establishment in CB-Aloha is also nonnegligible. The scheme selection largely influences performance in M2M communications. Some related works investigated the throughput and delay limits of these two mechanisms. In particular, [8] analyzed the optimal throughput of PB-Aloha and CB-Aloha, and showed that the throughput gain brought by connection establishment is significant. [9] conducted a comparative analysis of the throughput and delay limits between PB-Aloha and CB-Aloha. The beneficial connection establishment threshold in terms of optimal throughput and delay performance was discussed. However, these works ignore the energy constraints when exploring the performance limits, and the optimal configuration may be largely different when considering an energy-aware random access network, which might lead to higher energy consumption and a shorter lifetime of MTDs.

From the perspective of energy, the energy efficiency of PB-Aloha was optimized using numerical methods in [10]. Based on the framework in [11], [12] derived the energy efficiency limits and conducted a comprehensive analysis of PB-Aloha with the sleeping-awake scheme. The energy efficiency limits of CB-Aloha then largely remain unknown. Numerical methods were employed in [13] to further analyze and compare the energy efficiency of CB-Aloha and PB-Aloha. However, the numerical comparison in [13] assumes specific network parameter settings, such as constraining the data payload duration to one time slot.

Since the energy efficiency largely depends on the access protocols and transmission probability, a more reasonable comparison between PB-Aloha and CB-Aloha should be conducted in terms of optimal energy efficiency obtained by tuning transmission probability. This prompts us to characterize the optimal energy efficiency of CB-Aloha first, based on which the performance comparison is further conducted. The main contributions are outlined as follows:

- We accommodate the capability of CB-Aloha to transmit multiple data packets per transmission and propose lifetime throughput to characterize the energy efficiency. Then we derive the closed-form expression of the lifetime

Anshan Yuan and Xinghua Sun are with the School of Electronics and Communication Engineering, Sun Yat-sen University (Shenzhen Campus), Shenzhen 518107, China (e-mail: yuanansh@mail2.sysu.edu.cn; sunxinghua@mail.sysu.edu.cn)

Fangming Zhao is with the Zhejiang University–University of Illinois Urbana–Champaign Institute, Zhejiang University, Haining 314400, China (e-mail: fangming.23@intl.zju.edu.cn)

throughput, which integrates the node's lifetime, throughput, and energy consumption in each state.

- We conduct a comparative lifetime throughput analysis, and present the optimal operating region between PB-Aloha and CB-Aloha, which indicates that CB-Aloha outperforms PB-Aloha in energy efficiency when the network reaches saturation.
- Our analysis is also applied to the practical network case, i.e., grant-free 2-step RA-SDT schemes and grant-based 4-step RA-SDT schemes. We present the threshold for packet length that allows 4-step RA-SDT schemes to achieve a better lifetime throughput than 2-step RA-SDT.

The remainder of this letter is organized as follows. Section II presents the system model and preliminary analysis. Section III characterizes and optimizes the lifetime throughput of CB-Aloha and PB-Aloha. The comparative analysis is conducted and applied to the practical RA-SDT case in Section IV. Finally, Section V concludes the letter.

II. SYSTEM MODEL AND PRELIMINARY ANALYSIS

Consider a homogeneous slotted Aloha network¹ where n nodes communicate with a common receiver via a shared channel. Each node has an identical packet arrival rate and possesses an infinite-size buffer² to accommodate incoming packets. All nodes are synchronized, initiating transmissions only at the beginning of a time slot. Assume the collision model at the receiver, simultaneous transmissions by multiple nodes result in a collision, causing failure for all involved nodes. A transmission is successful only when there are no concurrent transmissions.

Fig.1 contrasts the transmission methodologies of PB-Aloha and CB-Aloha, employing superscript and subscript notations for clarity: N denotes CB-Aloha, and P represents PB-Aloha. In PB-Aloha, each node transmits a data packet with probability q when its buffer contains a packet, which lasts for one time slot, denoted as σ_P . When the transmission fails, the node retransmits the data packet with probability q in the next time slot. To standardize the transmission process, the time slot in PB-Aloha is determined by the data packet length.

Conversely, in CB-Aloha, each node sends a short length request (RTS) for channel competition, that lasts for σ_N with probability q to establish a connection once its buffer accumulates K data packets. Note that the length of RTS is smaller than the data packet, i.e., $\sigma_N < \sigma_P$, then the unit time slot length in CB-Aloha is determined by the length of RTS. A successful RTS reception prompts an acknowledgment (ACK) from the receiver, initiating the data packet transmission, and each transmission comprises K data packets transmission spanning M time slots and the signaling overhead lasting δ time slots. Failed attempts lead to retransmission of the RTS in the subsequent time slot with probability q .

The CB-Aloha can be analyzed by using a request-queue model [9]. As each node generates a request and competes

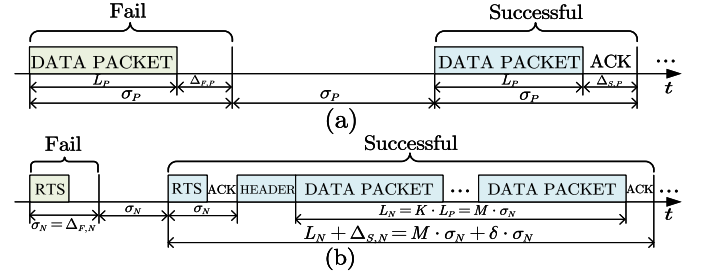


Fig. 1. Graphic illustration of (a) PB-Aloha. (b) CB-Aloha.

for the channel with this request, the network performance hinges on the aggregate behavior of the Head-Of-Line (HOL) request. By establishing the state transition process of each HOL request, the probability of successful HOL request transmission p_N in both saturated (i.e., each CB-Aloha node always has a packet to transmit) and unsaturated conditions has been characterized in [9] as:

$$p_N = \begin{cases} \exp\left(\mathbb{W}_0\left(-\frac{\hat{\lambda}_N}{M-\hat{\lambda}_N(M+\delta-1)}\right)\right) & \text{if } q \in \\ \left[-\frac{1}{n}\mathbb{W}_0\left(-\frac{\hat{\lambda}_N}{M-\hat{\lambda}_N(M+\delta-1)}\right), -\frac{1}{n}\mathbb{W}_{-1}\left(-\frac{\hat{\lambda}_N}{M-\hat{\lambda}_N(M+\delta-1)}\right)\right] & \\ \exp(-nq) & \text{otherwise,} \end{cases} \quad (1)$$

where $\mathbb{W}_0(\cdot)$ and $\mathbb{W}_{-1}(\cdot)$ are two branches of the Lambert \mathbb{W} function. The node throughput is given by [9]:

$$\lambda_{\text{out}}^N = \begin{cases} \lambda_N & \text{if } p_N \in S(p_N, \hat{\lambda}_N) \\ \frac{M}{-\frac{n}{p_N \ln p_N} + n(M+\delta-1)} & \text{otherwise,} \end{cases} \quad (2)$$

where

$$S(p_N, \hat{\lambda}_N) = \left\{ p_N : \exp\left(\mathbb{W}_{-1}\left(-\frac{\hat{\lambda}_N}{M-\hat{\lambda}_N(M+\delta-1)}\right)\right) < p_N < \exp\left(\mathbb{W}_0\left(-\frac{\hat{\lambda}_N}{M-\hat{\lambda}_N(M+\delta-1)}\right)\right) \right\}. \quad (3)$$

Assume that each node possesses an initial finite amount of energy E , consequently determining its finite lifetime. For homogeneous CB-Aloha, the expected lifetime T_N is identical for each node, in the unit of time slots. Throughout the lifetime, each node can exist in four states: (1) *failed state*, i.e., the node attempts to transmit a request but fails. (2) *successful state*, i.e., the node successfully transmits both request and data. (3) *waiting state*, i.e., the node holds one virtual HOL request, awaiting channel access. (4) *idle state*, i.e., the node's request queue is devoid of any pending requests.

Let n_W , n_I , n_F and n_S denote the expected number of requests for each node being in the waiting, idle, failed and successful state during its lifetime, respectively. The successful transmission state lasts for $M + \delta$ time slots while the other states just last for 1 time slot. The expected lifetime T_N , in the unit of time slots σ_N , can be written as:

$$T_N = n_I + n_W + n_F + n_S(M + \delta). \quad (4)$$

Let P_I , P_W , and P_T denote the normalized power consumption in the idle, waiting, and transmission states, respectively, as determined by the practical network configuration. Generally, we assume that $P_I = P_W \leq P_T$. According to the total energy constraint of each node, we have

$$P_W(n_I + n_W) + P_T(n_F + n_S(M + \delta)) = E/\sigma_N. \quad (5)$$

¹By using the methodology in [7], our model can be easily extended to the heterogeneous networks where nodes are divided into several groups according to distinct traffic characteristics and transmission probability.

²The performance is not sensitive to the buffer size when it is not too small.

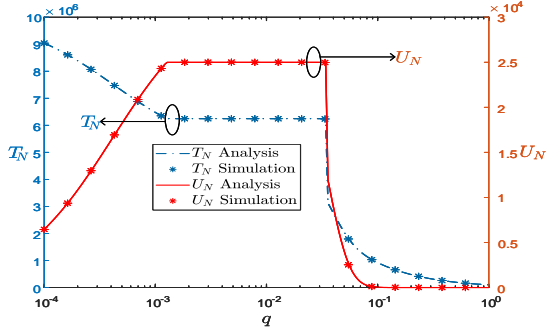


Fig. 2. Lifetime T_N and lifetime throughput U_N of each node, $n = 100$, $M = 8$, $\delta = 4$, $E/\sigma_N = 10^7$, $P_T = 100$, $P_W = 1$, $\lambda_N = 0.004$.

Due to the constraint of finite energy, each node has a restricted capacity to deliver packets throughout its lifetime. The lifetime throughput of each node U_N is defined as the average number of packets that a node can successfully transmit during its entire lifetime. In the following section, U_N will be characterized and further optimized.

III. LIFETIME THROUGHPUT LIMITS ANALYSIS

A. Lifetime Throughput limits in CB-Aloha

This subsection aims to obtain the maximum lifetime throughput of each CB-Aloha node $U_{\max}^{p,N}$. The lifetime throughput of each node U_N , can be written as:

$$U_N = \lambda_{\text{out}}^N T_N. \quad (6)$$

The following lemma presents the expression of the expected lifetime of each CB-Aloha node T_N .

Lemma 1: The expected lifetime of each node is given by

$$T_N = \begin{cases} \frac{E/\sigma_N}{\frac{(1+(M+\delta-1)p_L)\lambda_N}{M p_L} (P_T - P_W) + P_W} & \text{if } p_N \in S(p_N, \hat{\lambda}_N) \\ \frac{\frac{E}{\sigma_N} (1 - p_N \ln(p_N))(M + \delta - 1)}{P_W - \frac{(n-1)P_W + P_T}{M} (M + \delta - 1) p_N \ln(p_N) - \frac{(P_T - P_W) \ln p_N}{n}} & \text{otherwise,} \end{cases} \quad (7)$$

where $p_L = \exp\left(\mathbb{W}_0\left(-\frac{\hat{\lambda}_N}{M - \hat{\lambda}_N(M + \delta - 1)}\right)\right)$.

Proof: Please see Appendix A. ■

By combining (2), (6) and (7), the lifetime throughput of each node U_N is given by

$$U_N = \begin{cases} \frac{E/\sigma_N}{\frac{(1+(M+\delta-1)p_L)\lambda_N}{M p_L} (P_T - P_W) + P_W} & \text{if } p_N \in S(p_N, \hat{\lambda}_N) \\ \frac{E/\sigma_N}{\frac{(n-1)P_W + P_T}{M} (M + \delta - 1) + \frac{P_T - P_W}{M p_N} - \frac{n P_W}{M p_N \ln p_N}} & \text{otherwise.} \end{cases} \quad (8)$$

Fig. 2 shows the simulation results about lifetime T_N and lifetime throughput U_N versus transmission probability q of each node. Our simulation considers a $n = 100$ nodes CB-Aloha network where each node has Bernoulli packet arrival rate $\lambda_N = 0.004$. Given the power consumption P_T and P_W and a finite amount of energy normalized by time slot E/σ_N , we calculate the lifetime T_N and the average number of packets that a node can successfully transmit during its lifetime as their lifetime throughput U_N . Both simulations and the analytical result of Eq. (7) and Eq. (8) have shown that as q increases, T_N is non-increasing while U_N is non-monotonic, indicating a trade-off between T_N and U_N when q is small. We are interested in maximizing the lifetime throughput of each node U_N by tuning the transmission probability q . In practice, each node is expected to live longer than a certain threshold

value to avoid early death. Under such lifetime constraint, we have the following constrained optimization problem:

$$\begin{aligned} U_{\max}^{p,N} &= \max_q U_N \\ \text{s.t. } T_N &\geq T_0^N. \end{aligned} \quad (9)$$

The following theorem gives the solution to problem (9).

Theorem 1: Given the data length M , the maximum lifetime throughput $U_{\max}^{p,N} = \max_q U_N$ under the constraint of $T_N \geq T_0^N$ is given by

$$U_{\max}^{p,N} = \begin{cases} \frac{E/\sigma_N}{\frac{(1+(M+\delta-1)p_L)\lambda_N}{M p_L} (P_T - P_W) + P_W} & \text{if } \lambda_N \leq \lambda_M^N \text{ and } T_0^N \leq T_0^{*,N} \\ \frac{E/\sigma_N}{\frac{(n-1)P_W + P_T}{M} (M + \delta - 1) + \frac{P_T - P_W}{M p_m} - \frac{n P_W}{M p_m \ln p_m}} & \text{if } \lambda_N > \lambda_M^N \text{ and } T_0^N \leq T_0^{*,N} \\ \frac{E/\sigma_N}{\frac{(n-1)P_W + P_T}{M} (M + \delta - 1) + \frac{P_T - P_W}{M p_c^N} - \frac{n P_W}{M p_c^N \ln p_c^N}} & \text{if } T_0^{*,N} < T_0^N \leq \frac{E/\sigma_N}{P_W}, \end{cases} \quad (10)$$

otherwise, (9) has no feasible solution. The corresponding optimal transmission probability q_{\max}^N is set to be

$$q_{\max}^N = \begin{cases} \left[\frac{-\mathbb{W}_0\left(-\frac{\hat{\lambda}_N}{M - \hat{\lambda}_N(M + \delta - 1)}\right)}{n}, \frac{-\mathbb{W}_{-1}\left(-\frac{\hat{\lambda}_N}{M - \hat{\lambda}_N(M + \delta - 1)}\right)}{n} \right] & \text{if } \lambda_N \leq \lambda_M^N \text{ and } T_0^N \leq T_0^{*,N} \\ -(\ln p_m)/n & \text{if } \lambda_N > \lambda_M^N \text{ and } T_0^N \leq T_0^{*,N} \\ -(\ln p_c^N)/n & \text{if } T_0^{*,N} < T_0^N \leq \frac{E/\sigma_N}{P_W}. \end{cases} \quad (11)$$

where λ_M^N marks the boundary of the saturated region ($\lambda_N > \lambda_M^N$) and the unsaturated region ($\lambda_N \leq \lambda_M^N$) in CB-Aloha, which is given by

$$\lambda_M^N = \frac{M}{n} \frac{p_m \ln p_m}{p_m \ln p_m (M + \delta - 1) - 1}, \quad (12)$$

$T_0^{*,N}$ can be expressed as

$$T_0^{*,N} = \max\{T_N(p_L), T_N(p_m)\}, \quad (13)$$

p_m is given by

$$p_m = \exp\left(\frac{n - \sqrt{n^2 + 4n\left(\frac{P_T}{P_W} - 1\right)}}{2\left(\frac{P_T}{P_W} - 1\right)}\right), \quad (14)$$

and p_c^N is the solution of the following equation:

$$T_0^N = \frac{\frac{E}{\sigma_N} (1 - p_c^N \ln p_c^N) (M + \delta - 1)}{P_W - \frac{(n-1)P_W + P_T}{M} (M + \delta - 1) p_c^N \ln p_c^N - \frac{(P_T - P_W) \ln p_c^N}{n}}. \quad (15)$$

Proof: Please see Appendix B. ■

Fig. 3a depicts the maximum lifetime throughput $U_{\max}^{p,N}$ versus lifetime constraint T_0^N . It illustrates that when $T_0^N < T_0^{*,N}$, $U_{\max}^{p,N}$ is constant for T_0^N which aligns the case that without lifetime constraint. As $T_0^N > T_0^{*,N}$, $U_{\max}^{p,N}$ decreases when T_0^N increases and $U_{\max}^{p,N}$ is unaffected by the arrival rate λ_N since the network becomes saturated. Additionally, Fig. 3b indicates that the optimal transmission probability p_{\max}^N remains unchanged for $T_0^N < T_0^{*,N}$. Above $T_0^{*,N}$, or with higher transmission power consumption P_T , nodes lower their transmission probability q to meet the constraints, which results in an increased p_{\max}^N with higher T_0^N or P_T .

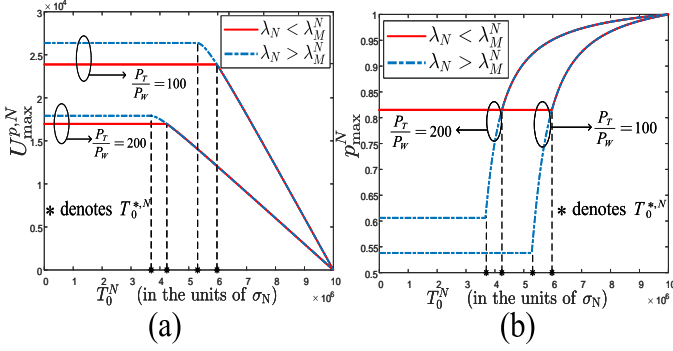


Fig. 3. The (a) maximum lifetime throughput $U_{\max}^{p,N}$ and (b) optimal successful transmission probability p_{\max}^N versus constraint T_0^N in different packet arrival rate λ_N , $n = 100$, $M = 6$, $\delta = 4$, $E/\sigma_N = 10^7$, $P_W = 1$.

B. Lifetime Throughput Limits in PB-Aloha

The lifetime throughput of PB-Aloha can be directly obtained by that of CB-Aloha. Specifically, in PB-Aloha, the data packet reduces to unit-time slot for each transmission, and there is no additional overhead required for establishing the connection. By substituting $M = 1$ and $\delta = 0$ into (7) and (8), the expected lifetime T_P and lifetime throughput U_P of each PB-Aloha node can be obtained as following:

$$T_P = \begin{cases} \frac{E/\sigma_P}{\frac{\lambda_P}{\exp(\mathbb{W}_0(-n\lambda_P))} (P_T - P_W) + P_W} & \text{if } p \in S(p, \hat{\lambda}_P) \\ \frac{E/\sigma_P}{P_W - \frac{(P_T - P_W) \ln p}{n}} & \text{otherwise,} \end{cases} \quad (16)$$

$$U_P = \begin{cases} \frac{E/\sigma_P}{\frac{(P_T - P_W)}{\exp(\mathbb{W}_0(-n\lambda_P))} + \lambda_P} + \frac{P_W}{\lambda_P} & \text{if } p \in S(p, \hat{\lambda}_P) \\ \frac{E/\sigma_P}{\frac{P_T - P_W}{p} - \frac{nP_W}{p \ln p}} & \text{otherwise,} \end{cases} \quad (17)$$

where

$$S(p, \hat{\lambda}_P) = \{p : \exp(\mathbb{W}_{-1}(-n\lambda_P)) < p < \exp(\mathbb{W}_0(-n\lambda_P))\}. \quad (18)$$

Therefore, the maximum lifetime throughput $U_{\max}^{p,P} = \max_q U_P$ under the constraint of $T_P \geq T_0^P$ is given by

$$U_{\max}^{p,P} = \begin{cases} \frac{E/\sigma_P}{\frac{(P_T - P_W)}{\exp(\mathbb{W}_0(-n\lambda_P))} + \lambda_P} + \frac{P_W}{\lambda_P} & \text{if } \lambda_P \leq \lambda_M^P \text{ and } T_0^P \leq T_0^{*,P} \\ \frac{E/\sigma_P}{\frac{(P_T - P_W)}{\exp(\mathbb{W}_0(-n\lambda_P))} + \lambda_P} + \frac{P_W}{\lambda_P} & \text{if } \lambda_P > \lambda_M^P \text{ and } T_0^P \leq T_0^{*,P} \\ \frac{E/\sigma_P}{\frac{P_T - P_W}{p_c^P} - \frac{nP_W}{p_c^P \ln p_c^P}} & \text{if } T_0^{*,P} < T_0^P \leq \frac{E/\sigma_P}{P_W}. \end{cases} \quad (19)$$

The corresponding optimal transmission probability q_{\max}^P is given by

$$q_{\max}^P = \begin{cases} [-\frac{1}{n}\mathbb{W}_0(-n\lambda_P), -\frac{1}{n}\mathbb{W}_{-1}(-n\lambda_P)] & \text{if } \lambda_P \leq \lambda_M^P \text{ and } T_0^P \leq T_0^{*,P} \\ -(\ln p_m)/n & \text{if } \lambda_P > \lambda_M^P \text{ and } T_0^P \leq T_0^{*,P} \\ -(\ln p_c^P)/n & \text{if } T_0^{*,P} < T_0^P \leq \frac{E/\sigma_P}{P_W}. \end{cases} \quad (20)$$

where λ_M^P marks the boundary of the saturated region ($\lambda_P > \lambda_M^P$) and the unsaturated region ($\lambda_P \leq \lambda_M^P$) in PB-Aloha, and can be expressed as

$$\lambda_M^P = \frac{\sqrt{1 + \frac{4}{n} \left(\frac{P_T}{P_W} - 1 \right)} - 1}{2 \left(\frac{P_T}{P_W} - 1 \right)} \exp \left\{ \frac{n - \sqrt{n^2 + 4n \left(\frac{P_T}{P_W} - 1 \right)}}{2 \left(\frac{P_T}{P_W} - 1 \right)} \right\}. \quad (21)$$

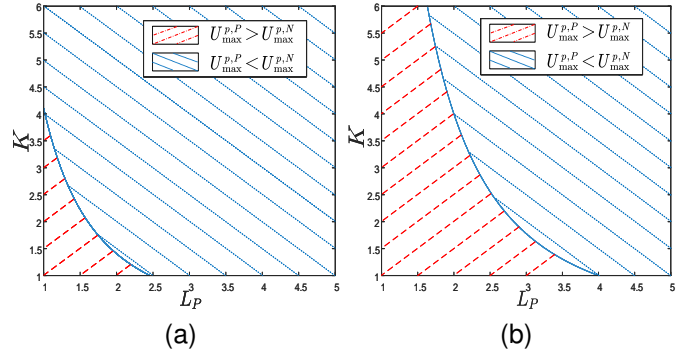


Fig. 4. Comparison about $U_{\max}^{p,P}$ and $U_{\max}^{p,N}$ in different K, L_P . $n = 100$, $\delta = 4$, $P_T = 100$, $P_W = 1$, $\Delta_{S,P} = 2$, $T_0^N = T_0^P = 0$, $\sigma_N = 2$, (a) Both networks are saturated. (b) Both networks are unsaturated.

$T_0^{*,P}$ can be expressed as

$$T_0^{*,P} = \frac{E/\sigma_P}{\frac{\min\{\lambda_P, \lambda_M^P\}}{\exp\{\mathbb{W}_0(-n \min\{\lambda_P, \lambda_M^P\})\}} (P_T - P_W) + P_W}, \quad (22)$$

p_m has been expressed in (14), and p_c^P is given by

$$p_c^P = \exp \left\{ -n \frac{\frac{E}{\sigma_P T_0^P} - P_W}{P_T - P_W} \right\}. \quad (23)$$

IV. ENERGY-AWARE M2M: CB-ALOHA OR PB-ALOHA

In this section, we will compare the optimal lifetime throughput of the CB-Aloha and PB-Aloha protocols to ascertain the optimal operating regime of these two schemes in energy-aware M2M communication.

A. Performance Comparison

As Fig. 1b illustrates, let L , Δ_S , and Δ_F denote the length of the data payload and the overhead time for each successfully or failed transmission. With CB-Aloha, the time wasted on unsuccessfully transmitting RTS is equal to σ_N , i.e. $\Delta_{F,N} = \sigma_N$. Fig. 1 also gives the relation between time slot and data length in PB-Aloha and CB-Aloha:

$$L_N = K \cdot L_P = M \cdot \sigma_N; \quad \sigma_P = L_P + \Delta_{S,P}, \quad (24)$$

where K is the number of the data length transmitted by PB-Aloha at one transmission. Due to the different slot length between σ_N and σ_P , when given λ_N , it is normalized by the time slot σ_N and subsequently rewritten in the unit of PB-Aloha time slot length σ_P , therefore, we have $\lambda_P = \lambda_N \frac{\sigma_P}{\sigma_N}$.

In the following, we will demonstrate the impact of K and L_P on the performance of CB-Aloha and PB-Aloha. Combining (10) and (19), when both networks are saturated and without life time constraint, we have $U_{\max}^{p,P} > U_{\max}^{p,N}$ if and only if the following inequality is satisfied:

$$\frac{KL_P(L_P + \Delta_{S,P}) - \sigma_N}{KL_P + \sigma_N(\delta - 1)} < \frac{((n-1)P_W + P_T)p_m \ln p_m}{(P_T - P_W) \ln p_m - nP_W}, \quad (25)$$

where p_m is given by (10). When both networks are unsaturated and without lifetime constraint, we have $U_{\max}^{p,P} > U_{\max}^{p,N}$ if and only if the following inequality is satisfied:

$$\frac{KL_P p_L (L_P + \Delta_{S,P})}{\sigma_N^2 + (KL_P + \sigma_N(\delta - 1))p_L \sigma_N} < \exp(\mathbb{W}_0(-n\lambda_P)), \quad (26)$$

where p_L is given by (7).

Compared to PB-Aloha, the transmission failures of CB-Aloha only involve RTS frames, at the cost of the overhead of connection establishment. However, the benefits brought by the reduction of transmission failure may not always outweigh the overhead, especially when there are few collisions in the network or the successful transmission time is small. As Fig. 4 illustrates, when both networks are unsaturated, nodes do not send data packets frequently, and there are few collisions in the networks. When K is small, i.e., the successful transmission time of CB-Aloha is small, $U_{\max}^{p,P} < U_{\max}^{p,N}$ only when L_P is large, where the packet transmission time of PB-Aloha is large and the energy wasting on failed transmission becomes high. As K grows, i.e., the successful transmission time of CB-Aloha increases, $U_{\max}^{p,P} < U_{\max}^{p,N}$ within a wider range of L_P value. When both networks are saturated, nodes frequently access the channel, resulting in more collisions. In this case, the region where $U_{\max}^{p,P} < U_{\max}^{p,N}$ has expanded compared to the unsaturated case.

B. Case Study: 4-step RA-SDT versus 2-step RA-SDT

To illustrate the practical application of the aforementioned analysis to real M2M networks, let's delve into the details of the 2-step RA-SDT and 4-step RA-SDT schemes, as outlined in the 3GPP Release 17 [3]. Detailed schematic diagrams and parameters setting of these two schemes are introduced in [9]: $\Delta_{S,P} = \Delta_{F,P} = 6\text{ms}$, $\Delta_{S,N} = 8\text{ms}$, $\sigma_N = 2\text{ms}$. By setting $P_T = 300\text{mW}$, $P_W = 3\text{mW}$, $n = 100$ and combining (24), (25) and (26), we can give the threshold K , denoted as K^* and L_P , denoted as L_P^* which enable $U_{\max}^{p,P} > U_{\max}^{p,N}$:

$$\begin{cases} L_N < \frac{8.9356}{L_P + 5.1774} & \text{when both networks are saturated,} \\ \frac{L_N p_L}{4 + 2p_L(L_N + 6)} < \frac{\exp(\mathbb{W}_0(-\lambda_N \frac{L_P + 6}{2}))}{L_P + 6} & \text{when both networks are unsaturated} \end{cases} \quad (27)$$

where p_L is given by (7).

When both networks are saturated and the data length of 2-step RA-SDT $L_P = 0.5\text{ms}$, for example, according to (27), we have $U_{\max}^{p,P} > U_{\max}^{p,N}$ as long as $L_N < 1.57\text{ms} \approx 3L_P$. It indicates that using the 4-step RA-SDT to transmit data of the same length as the 2-step RA-SDT will cause low energy efficiency. However, when $L_N > 1.57\text{ms}$, we have $U_{\max}^{p,N} > U_{\max}^{p,P}$, indicating that 4-step RA-SDT can improve energy efficiency by transmitting multiple packets during one connection which to some extent reduces the average overhead required to transmit each data packet.

V. CONCLUSION

This letter considers the energy efficiency optimization of Aloha networks with a finite battery budget. We derived closed-form expression of lifetime and lifetime throughput of CB-Aloha and PB-Aloha. The analysis reveals that there is a tradeoff between lifetime and lifetime throughput. We maximize lifetime throughput under lifetime constraints by tuning the channel access probability in CB-Aloha and PB-Aloha. We derive the optimal operating regime of these two schemes. Then, we apply our analysis to practical RA-SDT networks. Our analysis revealed that while the 4-step RA-SDT

increases overhead during frequent small data transmissions, it still enhances energy efficiency by enabling the transmission of multiple data packets within one connection.

APPENDIX A PROOF OF LEMMA 1

The transmission states can be divided into successful transmission states and failed states. Note that p_N denotes the probability of successful transmission. In each transmission attempt, with probability p_N , each node spends $M + \delta$ time slots in successful transmissions, and with probability $1 - p_N$, it spends one time slot in collision. So the number of the successful transmission state and failed state satisfies the following relation:

$$\frac{n_S}{n_F} = \frac{p_N}{1 - p_N}. \quad (28)$$

Since the CB-Aloha network can be analyzed by a request-queue model in [9], the mean request service rate of each node, μ_r , which is defined as a ratio of the number of successful requests and each node's lifetime, can be written as:

$$\mu_r = \frac{n_S}{n_W + n_F + n_S(M + \delta)}. \quad (29)$$

The offered load ρ of each node's data queue is then given by

$$\rho = \frac{\lambda_r}{\mu_r} = \frac{\lambda_N (n_W + n_F + n_S(M + \delta))}{M n_S}, \quad (30)$$

where λ_N is the packet arrival rate of each node. When the network is unsaturated with $\rho < 1$, the offered load equals the probability that the nodes' queue is not empty. We then have

$$\frac{n_W + n_F + n_S(M + \delta)}{n_I} = \frac{\rho}{1 - \rho}. \quad (31)$$

By combining (4), (5), (28), (30) and (31), the expected lifetime of each node T_N in unsaturated situation can be obtained. When the network becomes saturated with $\rho \geq 1$, we have $n_I = 0$. In this case, the mean service rate of each node's queue μ_r equals its throughput, then

$$\mu_r = \frac{p_N \ln p_N}{n p_N \ln p_N (M + \delta - 1) - n}. \quad (32)$$

By combining (4), (5), (28), (29) and (32), then T_N in saturated situation can be obtained.

APPENDIX B PROOF OF THEOREM 1

To get the optimal lifetime throughput with the lifetime constraint. We first propose a Lemma.

Lemma 2: The maximum lifetime throughput without any constraints $U_{\max}^{p,N,T_0=0}$ is given by

$$U_{\max}^{p,N,T_0=0} = \begin{cases} \frac{E/\sigma_N}{\frac{1+(M+\delta-1)p_L}{M p_L} (P_T - P_W) + \frac{P_W}{\lambda_N}} & \text{if } p_m \leq p_L \\ \frac{E/\sigma_N}{\frac{((n-1)P_W + P_T)(M+\delta-1)}{M} + \frac{P_T - P_W}{M p_m} - \frac{n P_W}{M p_m \ln p_m}} & \text{otherwise,} \end{cases} \quad (33)$$

$$\text{where } p_m = \exp \left\{ \frac{n - \sqrt{n^2 + 4n \left(\frac{P_T}{P_W} - 1 \right)}}{2 \left(\frac{P_T}{P_W} - 1 \right)} \right\}.$$

Proof: Let

$$f(p_N) = \frac{E/\sigma_N}{\frac{((n-1)P_W+P_T)(M+\delta-1)}{M} + \frac{P_T-P_W}{Mp_N} - \frac{nP_W}{Mp_N \ln p_N}}. \quad (34)$$

If $p_N \notin S(p_N, \hat{\lambda}_N)$, then we have $U_N = f(p_N)$. It can be proved that $f(p_N)$ monotonically increases as p_N increases if $p_N < p_m$, and monotonically decreases as p_N increases if $p_N > p_m$. $f(p_N)$ is then maximized when $p_N = p_m$. It is clear that if $\frac{\hat{\lambda}_N}{M-\hat{\lambda}_N(M+\delta-1)} \geq e^{-1}$, then the network will become saturated and U_N is maximized when $p_N = p_m$. In the following, we focus on the condition of $0 < \frac{\hat{\lambda}_N}{M-\hat{\lambda}_N(M+\delta-1)} < e^{-1}$. Notice that as $P_T \geq P_W$, we have $p_m \geq \exp\{-1\} \geq \exp\left(\mathbb{W}_{-1}\left(-\frac{\hat{\lambda}_N}{M-\hat{\lambda}_N(M+\delta-1)}\right)\right)$. We then divide the discussion into two cases:

Case 1: $p_m \leq \exp\left(\mathbb{W}_0\left(-\frac{\hat{\lambda}_N}{M-\hat{\lambda}_N(M+\delta-1)}\right)\right) = p_L$:

This condition is equivalent to $\lambda_N \leq \lambda_M^N$ according to (10). Due to the monotonicity of $f(p_N)$, we have $f(p_N)$ monotonically increases as p_N increases when $p_N < \exp\left(\mathbb{W}_{-1}\left(-\frac{\hat{\lambda}_N}{M-\hat{\lambda}_N(M+\delta-1)}\right)\right)$, and decreases as p_N increases when $p_N > \exp\left(\mathbb{W}_0\left(-\frac{\hat{\lambda}_N}{M-\hat{\lambda}_N(M+\delta-1)}\right)\right)$.

Note that:

$$\frac{E/\sigma_N}{\frac{1+(M+\delta-1)p_N}{Mp_N}(P_T-P_W) + \frac{P_W}{\lambda_N}} = f(p_N), \quad (35)$$

when

$$p_N = \exp\left(\mathbb{W}_0\left(-\frac{\hat{\lambda}_N}{M-\hat{\lambda}_N(M+\delta-1)}\right)\right) \quad (36)$$

or

$$p_N = \exp\left(\mathbb{W}_{-1}\left(-\frac{\hat{\lambda}_N}{M-\hat{\lambda}_N(M+\delta-1)}\right)\right), \quad (37)$$

and $\frac{E/\sigma_N}{\frac{1+(M+\delta-1)p_N}{Mp_N}(P_T-P_W) + \frac{P_W}{\lambda_N}}$ is a monotonically non-decreasing function of p_N . Therefore, U_N is maximized when $p_N = \exp\left(\mathbb{W}_0\left(-\frac{\hat{\lambda}_N}{M-\hat{\lambda}_N(M+\delta-1)}\right)\right)$.

Case 2: $p_m > \exp\left(\mathbb{W}_0\left(-\frac{\hat{\lambda}_N}{M-\hat{\lambda}_N(M+\delta-1)}\right)\right) = p_L$:

This condition is equivalent to $\lambda_N > \lambda_M^N$ according to (10). In this case, we have $U_N = f(p_N)$ if $p_N \notin S(p_N, \hat{\lambda}_N)$, which is maximized when $p_N = p_m$. If $p_N \in S(p_N, \hat{\lambda}_N)$, then we have $U_N < f(p_m)$. So U_N is maximized when $p_N = p_m$. ■

Now let us take into consideration the lifetime constraint of each CB-Aloha node $T_N \geq T_0^N$. According to (7), we have: $T_{\max}^N = \max_{p_N} T_N = \frac{E/\sigma_N}{P_W}$. If the lifetime constraint $T_0^N > \frac{E/\sigma_N}{P_W}$, then the optimization problem (9) is not feasible. If $P_T = P_W$, then we have $T_N = \frac{E/\sigma_N}{P_W}$ according to (7), in this case, if the lifetime constraint $T_0^N \leq \frac{E/\sigma_N}{P_W}$, then the optimization problem (9) becomes unconstrained optimization, and the solution is given by (33). When $P_T > P_W$ and $T_0^N \leq \frac{E/\sigma_N}{P_W}$, we divide the discussion into two cases:

Case 1: $p_m \leq \exp\left(\mathbb{W}_0\left(-\frac{\hat{\lambda}_N}{M-\hat{\lambda}_N(M+\delta-1)}\right)\right) = p_L$:

In this case, we have:

$$T_N(p_L) = \frac{E/\sigma_N}{\frac{1+(M+\delta-1)p_L}{Mp_L}\lambda_N(P_T-P_W) + P_W}, \quad (38)$$

according to Lemma 1, where $T_N(\cdot)$ is a function of p_N given by (7). If $T_0^N \leq T_N(p_L)$, then

$$p_N = \exp\left(\mathbb{W}_0\left(-\frac{\hat{\lambda}_N}{M-\hat{\lambda}_N(M+\delta-1)}\right)\right) \in \{p_N | T_0^N \leq T_N\}, \quad (39)$$

indicating that $p_N = \exp\left(\mathbb{W}_0\left(-\frac{\hat{\lambda}_N}{M-\hat{\lambda}_N(M+\delta-1)}\right)\right)$ lies in the feasible region of the optimization problem (9). According to Case 1 of the unconstrained optimization problem, we have:

$$U_{\max}^{p,N} = \frac{E/\sigma_N}{\frac{1+(M+\delta-1)\exp\left(\mathbb{W}_0\left(-\frac{\hat{\lambda}_N}{M-\hat{\lambda}_N(M+\delta-1)}\right)\right)}{M\exp\left(\mathbb{W}_0\left(-\frac{\hat{\lambda}_N}{M-\hat{\lambda}_N(M+\delta-1)}\right)\right)}(P_T-P_W) + \frac{P_W}{\lambda_N}} \quad (40)$$

which is achieved when $p_N = \exp\left(\mathbb{W}_0\left(-\frac{\hat{\lambda}_N}{M-\hat{\lambda}_N(M+\delta-1)}\right)\right)$.

If $T_0^N > T_N\left(\exp\left(\mathbb{W}_0\left(-\frac{\hat{\lambda}_N}{M-\hat{\lambda}_N(M+\delta-1)}\right)\right)\right) =$

$$\frac{E/\sigma_N}{\frac{1+(M+\delta-1)\exp\left(\mathbb{W}_0\left(-\frac{\hat{\lambda}_N}{M-\hat{\lambda}_N(M+\delta-1)}\right)\right)\lambda_N}{M\exp\left(\mathbb{W}_0\left(-\frac{\hat{\lambda}_N}{M-\hat{\lambda}_N(M+\delta-1)}\right)\right)}(P_T-P_W) + P_W}, \quad (41)$$

then $T_N \geq T_0^N$ is equivalent to $p_N \geq p_c^N > \exp\left(\mathbb{W}_0\left(-\frac{\hat{\lambda}_N}{M-\hat{\lambda}_N(M+\delta-1)}\right)\right)$, as T_N monotonically increases as p_N increases. As $p_m \leq \exp\left(\mathbb{W}_0\left(-\frac{\hat{\lambda}_N}{M-\hat{\lambda}_N(M+\delta-1)}\right)\right)$, U_N monotonically decreases as p_N increases when $p_N > \exp\left(\mathbb{W}_0\left(-\frac{\hat{\lambda}_N}{M-\hat{\lambda}_N(M+\delta-1)}\right)\right)$. As a result, we have:

$$U_{\max}^{p,N} = \frac{E/\sigma_N}{\frac{((n-1)P_W+P_T)(M+\delta-1)}{M} + \frac{P_T-P_W}{Mp_c} - \frac{nP_W}{Mp_c \ln p_c}}, \quad (42)$$

which is achieved when $p_N = p_c^N$. p_c^N is the solution of the equation (15).

Case 2: $p_m > \exp\left(\mathbb{W}_0\left(-\frac{\hat{\lambda}_N}{M-\hat{\lambda}_N(M+\delta-1)}\right)\right) = p_L$:

In this case, we have:

$$T_N(p_m) = \frac{\frac{E}{\sigma_N}(1-p_m \ln p_m(M+\delta-1))}{P_W - \frac{((n-1)P_W+P_T)(M+\delta-1)p_m \ln p_m}{n} - \frac{(P_T-P_W) \ln p_m}{n}}, \quad (43)$$

according to Lemma 1, if $T_0^N \leq T_N(p_m)$, then

$$p_N = p_m \in \{p_N | T_0^N \leq T_N\}, \quad (44)$$

indicating that $p_N = p_m$ lies in the feasible region of the optimization problem (9). According to Case 2 of the unconstrained optimization problem, we have:

$$U_{\max}^{p,N} = \frac{E/\sigma_N}{\frac{((n-1)P_W+P_T)(M+\delta-1)}{M} + \frac{P_T-P_W}{Mp_m} - \frac{nP_W}{Mp_m \ln p_m}}, \quad (45)$$

which is achieved when $p_N = p_m$. If $T_0^N > T_N(p_m)$, then $T_N \geq T_0^N$ is equivalent to $p_N \geq p_c^N > p_m$, as T_N monotonically increases as p_N increases. As $p_m > \exp\left(\mathbb{W}_0\left(-\frac{\hat{\lambda}_N}{M-\hat{\lambda}_N(M+\delta-1)}\right)\right)$, U_N monotonically decreases as p_N increases when $p_N > p_m$. As a result, we have:

$$U_{\max}^{p,N} = \frac{E/\sigma_N}{\frac{((n-1)P_W+P_T)(M+\delta-1)}{M} + \frac{P_T-P_W}{Mp_c} - \frac{nP_W}{Mp_c \ln p_c}}, \quad (46)$$

which is achieved when $p_N = p_c^N \cdot p_c^N$ is the solution of the equation (15). Then by using the explicit relation between p_N and q , we can easily obtain the optimal transmission probability q_{\max}^N , given by (11).

REFERENCES

- [1] D. López, A. De Domenico, N. Piovesan, G. Xinli, H. Bao, S. Qitao, and M. Debbah, "A Survey on 5G Radio Access Network Energy Efficiency: Massive MIMO, Lean Carrier Design, Sleep Modes, and Machine Learning," *IEEE Commun. Surveys Tuts.*, vol. 24, no. 1, pp. 653–697, 1st Quart., 2022.
- [2] R. Mahapatra, Y. Nijsure, G. Kaddoum, N. Ul Hassan, and C. Yuen, "Energy Efficiency Tradeoff Mechanism Towards Wireless Green Communication: A Survey," *IEEE Commun. Surveys Tuts.*, vol. 18, no. 1, pp. 686–705, 1st Quart., 2016.
- [3] *5G; NR; Medium Access Control (MAC) protocol specification (Release 17)*, document TS 38.321 V17.0.0, 3GPP, May 2022.
- [4] H. Kong, M. Lin, L. Han, W.-P. Zhu, Z. Ding, and M.-S. Alouini, "Uplink Multiple Access With Semi-Grant-Free Transmission in Integrated Satellite-Aerial-Terrestrial Networks," *IEEE J. Sel. Areas Commun.*, vol. 41, no. 6, pp. 1723–1736, June 2023.
- [5] Y. Guo, M. Lin, H. Kong, M. Cheng, and W.-P. Zhu, "NOMA Assisted Semi-Grant-Free Transmission Scheme in Satellite Systems," *IEEE Commun. Lett.*, vol. 27, no. 8, pp. 2122–2126, Aug. 2023.
- [6] Y. Gao, W. Zhan, and L. Dai, "Random Access: Connection-Free or Connection-Based?" in *From 5g To 6g and Beyond: The 7 Cs Of Future Communications*. World Scientific, 2023, pp. 105–140.
- [7] L. Dai, "A Theoretical Framework for Random Access: Stability Regions and Transmission Control," *IEEE/ACM Trans. Networking*, vol. 30, no. 5, pp. 2173–2200, Oct. 2022.
- [8] Y. Gao and L. Dai, "Random Access: Packet-Based or Connection-Based?" *IEEE Trans. Wireless Commun.*, vol. 18, no. 5, pp. 2664–2678, Mar. 2019.
- [9] X. Zhao and L. Dai, "Connection-Based Aloha: Modeling, Optimization, and Effects of Connection Establishment," *IEEE Trans. Wireless Commun.*, vol. 23, no. 2, pp. 1008–1023, Feb. 2024.
- [10] Z. Chen, Y. Feng, Z. Tian, Y. Jia, M. Wang, and T. Q. S. Quek, "Energy Efficiency Optimization for Irregular Repetition Slotted ALOHA-Based Massive Access," *IEEE Wireless Commun. Lett.*, vol. 11, no. 5, pp. 982–986, May 2022.
- [11] L. Dai, "Stability and Delay Analysis of Buffered Aloha Networks," *IEEE Trans. Wireless Commun.*, vol. 11, no. 8, pp. 2707–2719, Aug. 2012.
- [12] X. Sun, H. Zhang, W. Zhan, X. Wang, and X. Chen, "How to Survive 10 Years' Life Time for Machine Type Devices: A Study of Random Access With Sleeping-Awake Cycle," *IEEE Trans. Commun.*, vol. 71, no. 11, pp. 6727–6744, Nov. 2023.
- [13] H. Zhou, Y. Deng, L. Feltrin, and A. Höglund, "Analyzing Novel Grant-Based and Grant-Free Access Schemes for Small Data Transmission," *IEEE Trans. Commun.*, vol. 70, no. 4, pp. 2805–2819, Feb. 2022.